



STOCKHOLM UNIVERSITY
DEPARTMENT OF ASTRONOMY

BACHELOR OF SCIENCE THESIS

**A Dysonian Search for Kardashev Type III Civilisations in
Spiral Galaxies**

Author:
Per Calissendorff

Supervisor:
Erik Zackrisson

May 29, 2013

*“-This is Radio Nowhere. Is there anybody alive out there?
Is there anybody alive out there?”*

Bruce Springsteen, "Radio Nowhere" [Magic 2007]

Abstract

What would happen if a civilisation grows way beyond that of their own planet and solar system in terms of energy disposal? Such a civilisation may want to expand and develop stellar engineering on a galactic scale. If they are advanced enough to construct Dyson spheres around a significant number of stars in the galaxy in order to harness their power, they would disrupt the natural scaling laws between mass and luminosity for their host galaxy. A civilisation with such technology would make their galaxy show up as an outlier when using well-known scaling laws such as the Tully-Fisher relation.

Here, I utilize the Tully-Fisher relation on a number of 4859 spiral galaxies from the Spiral-Field galaxy I-band ++ catalogue by Springob et al. (2007) in order to search for these highly developed Kardashev type III civilisations. This is done by using a technique pioneered by Annis (1999) where outliers are determined when more than 75% of the outgoing light is blocked. I find in my search 13 candidates that require further investigation for a better perspective on these elusive entities. I also discuss the limitations of this technique to detect a galaxy with most of its outgoing light veiled from distant observers.

Acknowledgements

My greatest thanks goes to my supervisor Erik Zackrisson, for giving me the opportunity to work on such an indulging thesis and the very first Swedish *Searching for Extra Terrestrial Intelligence* (SETI) project. Also for providing me with many ideas and being able to answer any questions that I had, no matter how trivial, not to mention giving many constructive comments on my report.

Further more, a big thanks to my fellow students at the Department of Astronomy for putting up with my ranting and keeping me company on the "loft" of AlbaNova.

Contents

List of Figures	vi
List of Tables	vii
1 Introduction	1
1.1 SETI	2
1.2 The Kardashev Scale	5
1.3 Dyson Spheres	6
1.4 Previous work	8
1.5 The Tully-Fisher Relation	8
1.5.1 Baryonic Tully-Fisher Relation	9
2 Observational data	10
2.1 Subsamples	10
2.1.1 Selection criteria	10
2.1.2 Rotational velocities	11
2.1.3 Absolute Magnitude (r-band)	12
2.2 Main Sample	13
2.2.1 Selection criteria	13
2.2.2 HI-Linewidth	13
2.2.3 Absolute magnitude (I-band)	14
3 The search	15
3.1 r-band data	15
3.2 I-band data	15
3.3 Intrinsic scatter in the Tully-Fisher relation	18
3.3.1 Monte-Carlo simulation	19
3.4 Light obstruction	20
3.4.1 Detection prospects	21
4 Results	24
4.1 Subsample Outliers	24
4.2 Main Sample Outliers	24
4.3 Final Outliers	25
5 Conclusions	27
5.1 The rate of star-fed type III civilisations	27
5.2 Uncertainties	28

5.3 Discussion	29
5.4 Summary	31
A Final sample	33
B Galaxies	36
Bibliography	40

List of Figures

1.1	Dyson Sphere Concept	7
3.1	Subsample	16
3.2	Main sample (N=4859)	16
3.3	Main sample errorbar plot	17
3.4	Main sample (N = 4202)	18
3.5	Monte-Carlo simulation	19
3.6	Monte Carlo histogram	20
3.7	Light obscuring	21
3.8	Potential outliers	22
A.1	Final sample	34
A.2	Main sample parameters	35
B.1	NGC 7814	36
B.2	NGC 0660	36
B.3	NGC 1003	37
B.4	IC 2461	37
B.5	NGC 2841	37
B.6	NGC 4288	38
B.7	IC 3726	38
B.8	NGC 5900	38
B.9	NGC 5963	38
B.10	NGC 7177	39
B.11	NGC 7331	39
B.12	NGC 7339	39
B.13	M-258011	39

List of Tables

4.1	Sub sample outliers	24
4.2	Main sample outliers	25

Chapter 1

Introduction

One of mankind's most successful traits is her curiosity. It has led her to great discoveries, driven her to map the skies and even venture out into space to start exploring other worlds, like and unlike her own... Perhaps this last statement is a bit premature. We have yet to actually set foot on another planet but it certainly seems like an exciting next step and surely captivates the imagination of many. Just seeing the celestial wonders of the vast Universe entices the curious mind to ask the question; *Are we really alone?*

This question has yet to be answered, as we have neither found evidence of extraterrestrial life, nor have we thoroughly explored all of the observable Universe. If intelligent life is found beyond our solar system, cascades of more questions arise; *How intelligent are they? Where are they? How many are there? etc.*

I conduct this thesis as the final part of my Bachelor of Science education at the Department of Astronomy at Stockholm University. Here I perform a search trying to put an upper limit for the number of possible Kardashev type III civilisations in local disk galaxies.

In the introduction section, I bring some insight on the background history of what *Searching for Extraterrestrial Intelligence* (SETI) is and how it can be executed. I also explain what the Kardashev scale is and what feats are required to be acknowledged as a highly advanced extraterrestrial civilisation according to this scale. In the later parts of the chapter, I describe what a Dyson Sphere is and lastly explain the Tully-Fisher relation. In the second chapter, I explain how data was obtained and what criteria were used to limit the search. The obtained data and the limitations of the technique used are explored in the third chapter. Chapter four contains the findings and further details on the possible Kardashev type III candidates. The final results and uncertainties are discussed in chapter five.

1.1 SETI

People have pondered upon the idea of extraterrestrial intelligence for many years, even centuries, forming huge geometrical shapes and making enormous fires to try and get the attention of alien beings. Modern SETI however, had to await the initiation of radio astronomy and the discovery of the vacuum wavelength of the spectral line for neutral Hydrogen, commonly known as the 21-cm emission line. The wavelength translates into 1420 MHz when used as a frequency in radio astronomy. It was ushered by Cocconi & Morrison (1959) that this line could be used as a transmission signal due to being a "universal" frequency as HI is the most abundant element in our Universe. The microwave region is also rather quiet compared to the rest of the electromagnetic spectrum, making the 21 cm line prominent as an interstellar signal with relative low background and thus its reason of usage in the very first SETI observational experiment. Soon after Cocconi & Morrison (1959) published their article on interstellar communications in *Nature*, Frank Drake (1961) conducted the very first observational experiments on the subject with *Project Ozma*. The project used a radio telescope to examine the stars *Tau Ceti* and *Epsilon Eridani* near the 1420 MHz frequency.

During the time when the Ozma Project was implemented Drake wrote an equation for the estimation of the number of radio-communicative extraterrestrial civilisations in the Milky Way. The *Drake's Equation* summarises the main factors one has to ask themselves when considering other radio-communicative intelligent life.

$$N = R_* \cdot f_p \cdot n_e \cdot f_l \cdot f_i \cdot f_c \cdot L \quad (1.1)$$

Here N is the number of communicating civilisations within the Milky Way, R_* the average star formation rate in the Galaxy per year, f_p the fraction of those stars which have planets, n_e the average number of Earth-like planets or moons with liquid water which might support life within a solar system, f_l the fraction that of planets which can and actually harbours life, f_i the fraction of the developed life that further develops intelligent life, f_c the fraction of civilisations that develops technology enough to produce detectable signs of their existence into space and L the length of time for which such a civilisations produce their signals. The first 3 factors can be gained by observations but the latter ones yet remain uncertain and remain in the realm of speculation. The equation sole purpose is not to quantify the number of intelligent civilisations but more so a contemplation of what factors determine the odds of finding intelligent life.

In an attempt to get a signal to reach extraterrestrial civilisations, the most powerful broadcast ever deliberately beamed into space was made with the Arecibo Radio telescope in 1974. The transmission sent consisted of a simple, pictorial message, aimed

into the globular star cluster M13. The clusters is roughly 21,000 light-years from us and contains approximately 300,000 stars. The message consists of 1679 bits, arranged into 73 lines of 23 characters per line, which are both prime numbers and may help in decoding. The message contains, among other things, information on our solar system, graphic of a double helix symbolising DNA, a stick figure of a human and the numbers 1 to 10. Although it is unlikely that this short inquiry will prompt any replies, the experiment was useful in getting us to think about the difficulties of communicating across space. About 3 years after the Arecibo message was sent, NASA launched the Voyager spacecrafts. The Voyager program consists of 2 probes which are the farthest man-made objects and are still travelling farther away. Just like the Arecibo message, both Voyager probes carries with them information about Earth and the human race but in the form of pictures and music instead of binary code.

Over a decade after Project Ozma, in the late 1970's the *Search for Extraterrestrial Radio Emissions from Nearby Developed Intelligent Populations* (SERENDIP) program was born at the University of California, Berkely (Tarter 2001). SERENDIP systems operate under a commensal search paradigm in which other radio telescopes' data and signals are processed in real-time. Although this means that the SERENDIP program does not selectively choose its own targets to look at or which frequencies to receive with, it keeps the costs down and can operate frequently. It is mainly used to look for interesting signs of extraterrestrial candidates which are later followed up using targeted searches with dedicated telescopes for verification. Interesting signs include signals with events above 60 times the average spectrum power, sets of 3 or more events recorded over a short period of time and 2 or more events with equal frequency in any rest frame at different times (Bowyer et al. 1993). Several SERENDIP projects have been launched, the most recent one is the SERENDIP V.v installed on the Arecibo Observatory in 2009 and is still operating (Bowyer 2011).

One of the larger SETI projects was the *Phoenix Project* which was ongoing from 1995 to 2004 (Project Phoenix Team, Backus et al. 2004). NASA had intentions to make a 10-year targeted search for SETI a few years earlier, but the project was cancelled due to budget reasons. Alas, from the ashes rose the Phoenix and became the most sensitive and systematic SETI search of that time as it picked up the very same equipment developed for the NASA SETI search. Three campaigns were conducted during Project Phoenix, first one Parkes, Australia in 1996 followed by 2 years at Green Bank, West Virginia, USA from 1996 to 1998. The last observations were done at Arecibo, Puerto Rico, USA from 1998 to 2004. The searches were performed by pointing telescopes at selected nearby stars, achieving high sensitivity even to weak signals. The Phoenix could also process data immediately so that within minutes of the original data collection a follow-up on any candidate signal could be made. Project Phoenix observed over 800

stars with distances up to circa 240 light years, however no extraterrestrial signals were confirmed.

The non-profit SETI League began a project called Argus in 1996 as an attempt to resurrect the all-sky survey component of the NASA SETI effort. Project Argus is named after the mythical Greek guard-beast who had 100 eyes and could see in all directions at once, which is just what the project seeks to do. By connecting thousands of small radio telescopes around the world online, they would be able to look at all direction at once in real time. The telescopes need not be very advanced and can be operated by dedicated amateur radio astronomers. The goal of Argus is to have about 5000 antennas which is required in order to achieve a continuous full sky view, and monitoring constantly so that no signal towards Earth would be missed. As of the year 2011, the Argus Project has only 144 stations in 27 different countries and too has yet failed to detect any conclusive evidence of ETI (Shuch 2011). A similar SETI project where many volunteers help out all around the globe is the SETI@home. By exploiting the SERENDIP at the Arecibo and connecting millions of computers online using the Internet, a combined super-computer can crunch the data and announce if any interesting signals have been detected that require follow-up observations.

Searching for intelligent life outside our planetary system becomes increasingly difficult with distance. A targeted microwave search where one looks at one object at a time at current sensitivity could detect the power equal of a TV transmission at a distance of 1 light year, within which there are no other solar systems. If an extraterrestrial civilisation was equipped with something equal to the strongest generated microwave signal on Earth (Arecibo Planetary Radar), they would be detected at a distance up to 3000 ly (Tarter 2001). The Sun's distance to the galactic center is about 27000 light years and the Milky Way has a diameter of about 110000 light years, meaning a civilisation as such would not be detected if on the other side of the Galaxy. Going through every single star in a targeted search is quite time consuming as well, so in order to go about that one can make a fully sky survey instead. The advantage of looking at a full sky view comes at a cost of detection range of about 2 orders of magnitude, meaning a civilisation similar to our own technological status would have to be rather close in order for us to detect them. Because of the limitation on our capabilities to send and detect extraterrestrial signals, most SETI work is done within the Milky Way. Here in my thesis however, the search goes way beyond that in order to find highly technological super advanced extragalactic civilisations. These civilisations have been given the name of *Kardashev Type III Civilisations*.

1.2 The Kardashev Scale

The Kardashev scale is a measurement of how much energy a technological civilisation has at its disposal and suggests its level of technological advancement. A scale of 3 types was suggested by the Soviet astrophysicist Nicolai Kardashev(1964).

- I** - Technological level close to the level presently attained on the Earth, with energy consumption at $\approx 4 \times 10^{19}$ erg/sec.
- II** - A civilisation capable of harnessing the energy radiated by its own star with energy consumption at $\approx 4 \times 10^{33}$ erg/sec.
- III** - A civilisation in possession of energy on the scale of its own galaxy, with energy consumption at $\approx 4 \times 10^{44}$ erg/sec.

Different scales have been suggested by others such as Carl Sagan where intermediate values are gained from extrapolates and interpolates of the values above. A formula for such purpose was presented as such:

$$K = \frac{\log_{10} MW}{10} \quad (1.2)$$

where K is the value of the civilisations' Kardashev rating and MW is the power it uses in measures of megawatts. As a simple comparison, the total world energy consumption on Earth in 2010 was about 500 exajoules, equal to an average power of 1.58×10^{13} W. This would make us land on approximately 0.72 on the Kardashev scale. It has been suggested that with the current energy consumption and technology growth there would be an additional 100-200 years before we would reach a rating such as that of a Kardashev type I.

Just having a high enough energy consumption would not be enough to define an advanced civilisation though. To maintain such a feat their growth must be faster than the frequency of life threatening disasters such as volcanoes, comets and climate changes such as an ice age. They must therefore learn to within time master space travel and even to modify the climate. These are just a few things that an advanced civilisation bump into during their transitions through the scale ranks. Some of them may seem quite far away from us to attain at current means but the seeds of a Type I civilisation are starting to show. A planetary communication system such as the Internet is a stepping stone for one.

The transition from a Type I to a Type II is a crucial step for any civilisation that attempts to strive on once their planet's energy sources becomes exhausted and would

require mastering the art of interplanetary travels, communications and stellar engineering. Further away on the scale is the type III civilisation which must be in possession of interstellar travels, interstellar communications and galactic engineering. No real reference has been obtained for such an advanced civilisation yet, but there are means to achieve such status. One approach is to gather high enough energy to rival that of the entire hosting galaxy by enclosing most stars within *Dyson spheres*.

1.3 Dyson Spheres

The creation of a spherical structure the size of a planetary orbit was suggested by Freeman Dyson (1960) when he published his paper in *Science*. The concept is to manufacture solar powered satellites that encompass a star in order to capture its energy output. Several variations of the Dyson sphere has been suggested such as a ring or a swarm of satellites around the targeted star. The most energy efficient one would be to completely encase the star in a complete shell. By harnessing most of the entire energy output of the star, the Dyson Sphere satellites would have to radiate the excessive heat in order not to melt. Using Stefan Boltzmann's law one can assert the surface temperature of a Dyson Sphere depending on its size.

$$T = \left(\frac{L}{4\pi R^2 \epsilon \sigma}\right)^{1/4} \quad (1.3)$$

Here T is the apparent temperature, L the energy output of the star, R the radius of the sphere, ϵ the emissivity of the material (relative ability to emit energy by radiation, equal to 1 for perfect black bodies and lower for real objects) and σ the Stefan Boltzmann constant ($\sigma = 1.38 \times 10^{-23} \text{J K}^{-1}$). Assuming a star similar to our own Sun and a radius of 1 AU, the apparent temperature would be somewhere between 200 to 300 K. This would correspond to a wavelength in the infrared and predicted to have a peak at around $10\mu\text{m}$.

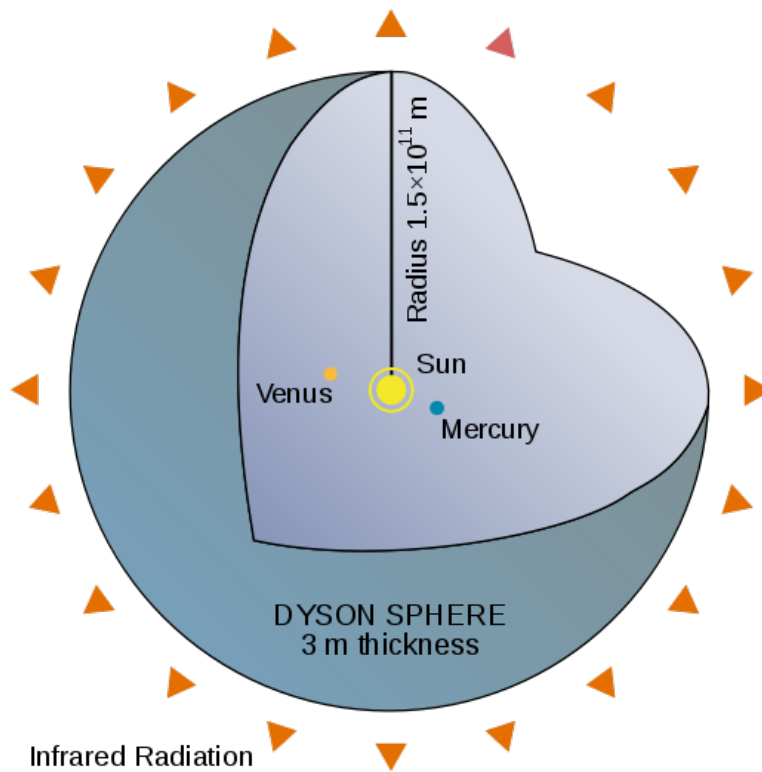


FIGURE 1.1: A simple illustrative Dyson sphere at 1 AU radius enclosing the Sun and nearby planets. The thickness is calculated by using the mass of elements heavier than Hydrogen taken from Jupiter.

One way to go about building a Dyson sphere would be to create self-replicating robots, or *von Neumann probes* (Freitas 1980), named after the Hungarian-American mathematician who calculated the possibility of self-replicating automatons. By sending these robots to mineral rich moons, they would manufacture factories to mass-produce copies of themselves. A moon is an ideal place for such probes as they could easily land and take off from it and be safe from erosion. As they go on reproducing more and more self replicating probes they would eventually move on and be used to build the Dyson sphere. Von Neumann probes are excellent in that sense to explore the Universe, spreading around similar to a virus in a body. What this means for a Type III civilisation that have been producing von Neumann probes for some time is that most of their galaxy's stars are covered in Dyson spheres. By blocking out the stars, the galaxy becomes dimmer in optical light and the mass to light ratio of the galaxy would then be lower than expected.

A large survey searching for Dyson spheres within the Galaxy was carried out by Carrigan (2009). It resulted in just a few quasi-plausible objects with the sought attributes

of Dyson spheres in a full-sky view of over 250,000 infrared sources.

1.4 Previous work

A small-scaled search for Kardashev type III civilisations has been carried out before by Annis (1999). He looked at a sample of 31 spiral galaxies in a *Tully-Fisher diagram* where the absolute magnitude is plotted against the rotational velocity of the galaxies. He suggested that objects 75% less luminous (i.e. a drop in 1.5 absolute magnitude) than the TFR should be considered as an outlier and possible Kardashev type III candidate. No such outlier 1.5 absolute magnitudes below the relation was found in that survey. However, the same constraints for outliers as Annis (1999) imposed are followed here, so that a comparison can be made more easily. The ambition here is to enforce a stronger upper limit for the expected number of type III Kardashev civilisations than that what was earlier made.

1.5 The Tully-Fisher Relation

The empirical relationship between rotational velocity and absolute magnitude (or luminosity) for spiral disk galaxies is well known. The relation was first used as a distance indicator acquired by Tully & Fisher (1977) but can also be used to constrain models of disk galaxy formations. It can be derived by applying the *virial theorem* on a self-gravitating system where the gravitational potential energy is equal to the kinetic energy

$$\frac{GMm}{R} = \frac{mV^2}{2}$$

where M is the mass of the system, G the gravitational constant, V the rotational velocity and R the radius of the system. We then get a relation for the mass and rotational velocity as

$$M \propto V^2 R.$$

If we also assume that the mass has a dependency of typical mass-to-light ratio for stellar types, we get that mass is related to luminosity as

$$M = L \times (M/L).$$

The surface brightness of the system can be expressed as

$$I = \frac{L}{4\pi R^2} \quad \text{so that} \quad R \propto (L/I)^{1/2}$$

where I is the intensity of power transferred per area. Combining these equations we get

$$M = L \times (M/L) \propto RV^2 \propto (L/I)^{1/2}V^2$$

and solving for L yields

$$L \propto V^4.$$

This idealized relation between luminosity and rotational velocity is not perfectly obeyed in reality and is usually replaced by

$$L \propto V^\alpha$$

where α is a constant depending on the filter measured with, close to 4 when measuring in the I-band.

Depending on the literature and observed data, the Tully-Fisher relations may look a bit different. Changes can occur due the morphology (i.e. Hubble type) of the galaxies in the sample it was deduced from and also at what wavelength the data was obtained with. The one adopted here was derived by Masters et al. (2006):

$$M_I - 5 \log(h) = -7.85[\log(W_{\text{TF}}) - 2.5] - 20.85 \quad (1.4)$$

where M_I is the absolute magnitude in the I-band, W_{TF} is the rotational linewidth and h is the *Hubble constant*, H_0 divided by 100 km s⁻¹ Mpc⁻¹.

1.5.1 Baryonic Tully-Fisher Relation

Since the mass of a galaxy is proportional to the luminosity, the normal Tully-Fisher diagram can be represented as stellar mass vs. rotational velocity instead. Adding the mass of the gas in the galaxy rather than just the stellar part, a *Baryonic Tully-Fisher* relation can be derived. Doing so for low mass galaxies which are more rich in gas, the intrinsic scatter gets reduced (McGaugh 2000). Using the Baryonic Tully-Fisher relation might have aided in determining outliers in our search, but data for such was rather scarce and left for another time.

Chapter 2

Observational data

Data for the research was obtained from the literature on the Tully-Fisher relation for disk galaxies. The literature and its data were examined and assigned into two categories as some surveys were made by using different band filters and different ways of calculating the rotational speed of the galaxies. The categories were merged into one I-band sample consisting of the newer Spiral Field *I*-band (SFI++; Springob et al. 2005) catalogue which is used as the main sample here, and one r-band survey containing the data from Reyes et al. (2011) which serves as a smaller subsample. The subsample survey is not really competitive to the main sample SFI++ catalogue, but it serves as a consistency check of the results.

2.1 Subsamples

In their survey, Reyes et al. (2011) compiled their data from an earlier investigation in addition to new observations. The Apache Point Observatory 3.5-meter telescope was used to observe 95 galaxies with the addition of 94 galaxies from Pizagno et al. (2007), resulting in 189 objects. All the galaxies were observed in the photometric r-band.

2.1.1 Selection criteria

The Reyes et al. (2011) sample was selected using the following criteria:

- (i) $0.02 < z < 0.10$
- (ii) $-22.5 < M_r < -18.0$
- (iii) $f_{obs}(H_\alpha) > 2 \times 10^{-16} \text{erg s}^{-1} \text{cm}^{-2}$

$$(iv) \quad 0.5 < n_s < 5.9 \quad \text{and} \quad n_s < 1.7 - (M_r + 18.0)$$

$$(v) \quad \log\left(\frac{[\text{OIII}]5007}{\text{H}\beta}\right) < \frac{0.61}{\log([\text{NII}]6583/\text{H}\alpha) - 0.47} + 1.19$$

Here z is the redshift, M_r the absolute magnitude in the r-band, f_{obs} the observed $H\alpha$ flux and n_s the *Sérsic index*.

The lower redshift limit (i) was introduced in order to ensure that the uncertainty in the absolute magnitude due to peculiar velocities would stay low. The upper redshift limit is a practical choice given the angular resolution required to obtain resolved rotation curves. The second (ii) cut to the absolute magnitude at the bright end would help to exclude non-star-forming (i.e. elliptical) galaxies that may have contaminated the sample. It should be added that the data from the Pizagno et al. (2007) survey had very similar absolute magnitude limits at -22 and -18.5. The $H\alpha$ flux cut (iii) was also meant to remove non-star-forming galaxy populations. The fourth (iv) cut to the Sérsic index limits the shape of the surface brightness profile. The fifth (v) excludes any *Active Galactic Nuclei*, *AGN*, this was made to ensure that the observed $H\alpha$ flux came from the disk and not the central AGN engine.

2.1.2 Rotational velocities

A spiral galaxy reaches its maximum rotational velocity at about 80% of its maximum radius and can be closely approximated with the shape of an arctangent model (Rubin et al. 1985). The observed disk galaxy rotation curves for the Reyes sample was obtained using an arctangent model derived by Courteau (1997).

$$V_{mod}(r) = V_0 + \frac{2}{\pi} V_{c,obs} \arctan\left(\frac{r}{R_{TO}}\right) \quad (2.1)$$

The model has 4 free parameters: the systematic or central velocity V_0 , the asymptotic circular velocity $V_{c,obs}$, the radius r and the turn-over radius where the rotation curve starts to flatten out R_{TO} . Velocity parameters were gained by using a Levenberg-Marquardt least square minimization routine on the observed $H\alpha$ flux. The rotational velocities were then corrected to edge-on orientation by

$$V_{corr} = V_{mod} / \sin \theta \quad (2.2)$$

where θ is the inclination calculated using

$$\sin \theta = \left(\frac{1 - q_d^2}{1 - q_z^2}\right)^{1/2}. \quad (2.3)$$

Here q_z is the disk thickness set to 0.19 as suggested by Haynes & Giovanelli (1984) and q_d is the axial ratio calculated as minor axis over major axis, b/a . An axial ratio of 0.19 or less would indicate a very high inclination, set to $\theta = 90^\circ$ and the object would be considered as edge-on already.

Errors for the rotational velocities were then calculated using error propagation, adding the systematic uncertainties and the inclination correction afterwards. The errors were largely dominated by the errors from the formal fit (i.e the shape of the rotation curve).

$$(\delta V_{80})^2 = \sum_{ij} \left(\frac{\partial V(R)}{\partial a_i} \right) \left(\frac{\partial V(R)}{\partial a_j} \right) \mathbf{C}_{ij} \Big|_{R=R_{80}} + \left(V_{80} - V_{80}^{(r)} \right)^2 + (\delta(\sin \theta))^2. \quad (2.4)$$

Here, $V(r)$ is the arctangent model function, a_i is the fit parameters, \mathbf{C}_{ij} the covariance matrix, $V_{80}^{(r)}$ the velocity amplitude at R_{80} and $\delta(\sin \theta)$ the inclination error in q_d .

2.1.3 Absolute Magnitude (r-band)

Disk galaxies are affected by dust obscuration, so that an inclined disk galaxy appears fainter and redder than if it were face-on (Burstein, Haynes and Faber 1991). An internal extinction correction to the absolute magnitude and colour of galaxies is then required to get the unobscured value. Here, the extinction in the λ filter is calculated based on the prescription of Tully et al. (1998):

$$A_\lambda^{\theta-0} = -\gamma_\lambda (M_\lambda^{\text{NC}}) \times \log(q_d) \quad (2.5)$$

where $A_\lambda^{\theta-0}$ represents a correction to a face-on orientation, q_d is the axial ratio of the disk, M_λ^{NC} is the Petrosian absolute magnitude uncorrected for internal extinction and γ_λ is a linear function of M_λ increasing for high luminous galaxies.

The final internal extinction-corrected absolute magnitude M_λ is then calculated as

$$M_\lambda = m_{\text{P},\lambda} - 5 \log(D_L/10\text{pc}) - K_\lambda - A_\lambda^{\text{MW}} - A_\lambda^{\theta-0}. \quad (2.6)$$

Here, $m_{\text{P},\lambda}$ is the apparent SDSS Petrosian magnitude in the wavelength λ in which galaxy fluxes are measured within a circular aperture. The radius of the aperture is defined by the shape of the azimuthally averaged light profile. D_L is the luminosity distance calculated from the redshift (with cosmology $\Omega_m = 0.3$, $\Omega_\Lambda = 0.7$ and $h = 0.7$). K_λ is the k -correction to $z = 0$ in order to get the quantity of light of the objects to be converted into their rest frames. A_λ^{MW} is the correction for Galactic extinction based on dust maps of Schlegel et al. (1998).

The uncertainty in M_λ was estimated to be

$$(\delta M_\lambda)^2 = (\delta m_{P,\lambda})^2 + \left(\frac{5}{\ln 10} \frac{\delta V_{\text{pec}}}{cz} \right)^2 + \left(\delta A_\lambda^{\theta=0} \right)^2. \quad (2.7)$$

Smaller uncertainties from redshift and Galactic extinction correction were neglected. The distance uncertainty was set to $\delta V_{\text{pec}} = 300 \text{ km s}^{-1}$, which is the typical amplitude of small-scale peculiar velocities for nearby galaxies (Strauss & Willick 1995) and the dominating one in this case.

2.2 Main Sample

The largest sample and therefore main sample of data came from the Springob et al. (2007) survey. The data consists of 4861 field and cluster disk galaxies from the SFI++ catalogue, composed of previous data from the Spiral Field I -band (SFI; Giovanelli et al. 1994), Spiral Cluster I -band 1 (SCI; Giovanelli et al. 1997) and Spiral Cluster I -band 2 (SC2; Dale et al. 1999) with both spectroscopy and photometry taken by several observatories.

2.2.1 Selection criteria

The various surveys composing the SFI++ catalogue had different criteria for their compilations. 2000 objects were observed using a limited apparent magnitude of < 14.5 , with a distance limit of < 100 Mpc. Other objects were found at fainter apparent magnitude and greater distances using different catalogues and new observations.

2.2.2 HI-Linewidth

Rotational velocity in the main sample was obtained using the *Doppler broadening* effect of the HI 21 cm line spectrum for each galaxy. This rotational velocity is usually referred to as velocity linewidth, W , and was corrected for instrumental and noise effects as described by Springob et al. (2005). Adding corrections for inclination and cosmic distance, the corrected HI line widths W_{21} are formed by:

$$W_{21} = \left(\frac{W_{\text{obs},21} - \Delta_s}{1+z} - \Delta_t \right) \frac{1}{\sin i}. \quad (2.8)$$

Here, $W_{\text{obs},21}$ is the observed width, Δ_t the turbulence correction set to $\Delta_t = 6.5 \text{ km s}^{-1}$, Δ_s the instrumental correction, z the redshift and i the inclination angle. The inclination

angle i is defined as

$$i = \cos^{-1} \sqrt{\frac{(b/a)^2 - q_0^2}{1 - q_0^2}} \quad (2.9)$$

where a and b are the observed semi-major and minor axis of the galaxy gained from isophote fitting and q_0 the intrinsic axial ratio of the disk. q_0 is appointed to 0.13 for morphological Hubble types Sbc and later, and to 0.2 for earlier types. An axis ratio of $b/a < 0.13$ would mean that the inclination is 90° and the galaxy viewed close to, or precisely edge-on.

2.2.3 Absolute magnitude (I-band)

To estimate extinction within the targeted galaxies themselves, the following equation from Giovanelli et al. (1994) was used:

$$\Delta M = -\gamma \log(a/b) \quad (2.10)$$

Here ΔM is the extinction in magnitudes, a and b are the observed semi-major and minor axis and γ is a quantity that depends on the galaxy's inferred absolute magnitude. γ ranges from 0.5 for faint galaxies $M_I > -19$ to 1.3 for bright $M_I < -22$ as shown by Giovanelli et al. (1994). Extinction from our Galaxy was made using values taken from the Diffuse Infrared Background experiment on *COBE* (Schlegel et al. 1998).

Chapter 3

The search

In this chapter the data is plotted in Tully-Fisher diagrams, where the Tully-Fisher relation is indicated by a red line. An additional green line is plotted 1.5 magnitudes below the TFR to denote where outliers are found. I also explore what the sensitivity of the observations meant for the search and further investigate the limitations of the technique used to find outliers.

3.1 r-band data

Because of the maximum absolute magnitude criteria of $M_r < -18$, any objects 1.5 magnitudes less luminous than the TFR at $\log_{10}[V_{80}] < 1.96$ would not be included in the survey. Therefore, the Reyes (2011) data sample got an additional pruning for all $\log_{10}[V_{80}] < 1.96$. The black dashed line in Fig. 3.1 shows the absolute magnitude limit which caused the additional minimum velocity (i.e mass) restraint. Out of the original 189 galaxies, 16 were removed from the sample for this reason. A linear least square fit was made instead of using the TFR Equation 1.5 because the appropriate values for it were not available in the paper. From the Reyes (2011) data, 2 outliers were found below the designated outlier line.

3.2 I-band data

Tully-Fisher diagrams of the main sample from the SFI++ catalogue are shown without errorbars in Fig. 3.2 and with errorbars in Fig. 3.3.

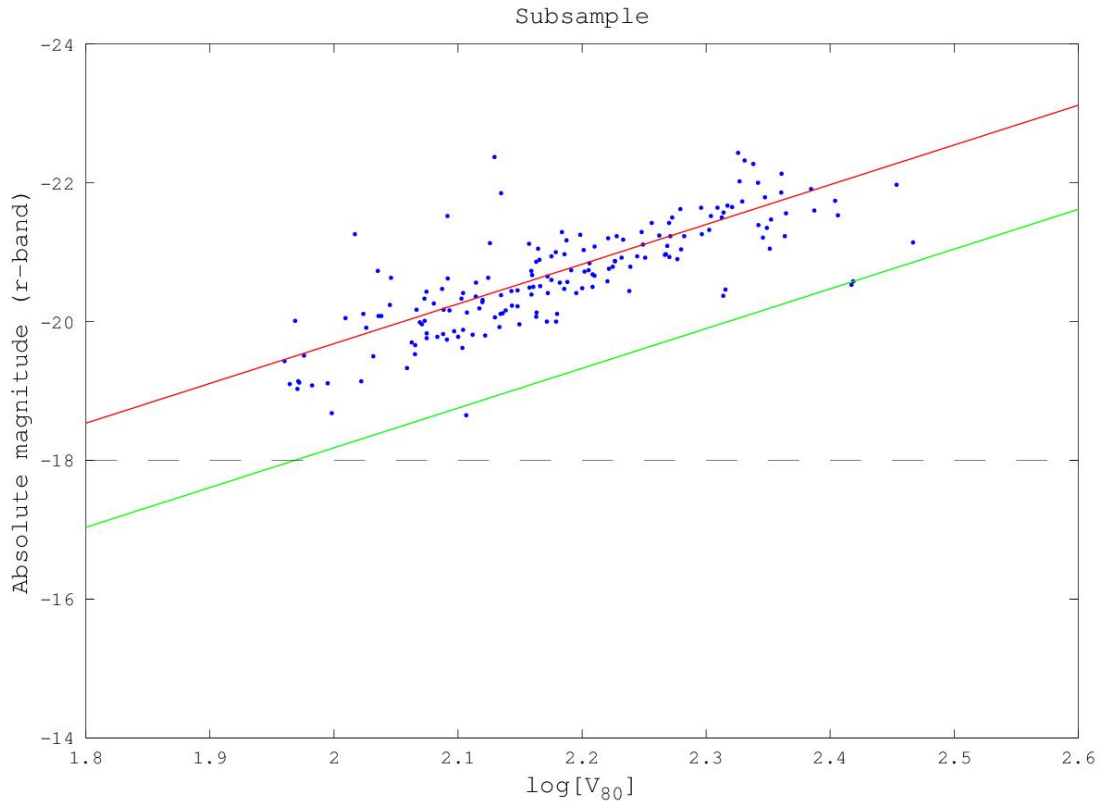


FIGURE 3.1: Plot of the subsample from Reyes (2011). Objects with $\log V_{80} < 1.96$ were removed and the black dashed line displays the maximum absolute magnitude limit. The red and green lines displays the linear fit and the outlier line.

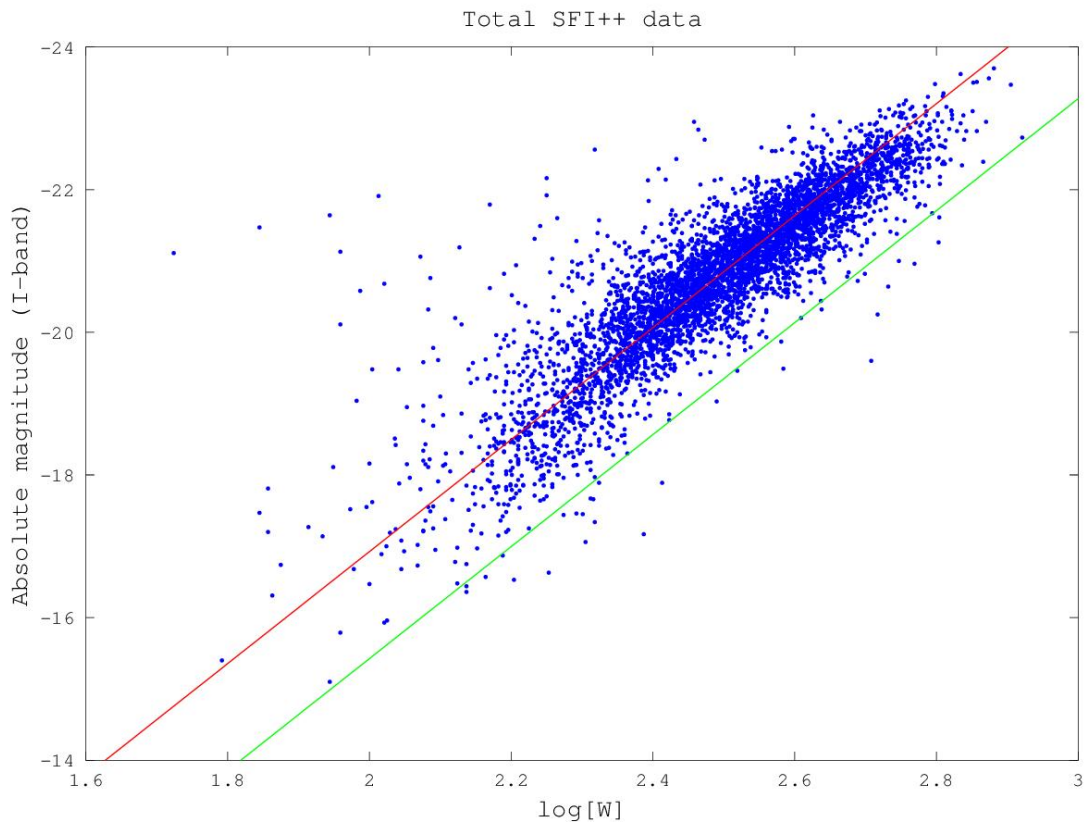


FIGURE 3.2: Plot of the main sample data from Springob et al. (2009) SFI++ catalogue. The Tully-Fisher relation is displayed as the red line. The green line 1.5 magnitudes below displays the limit for where outliers are found.

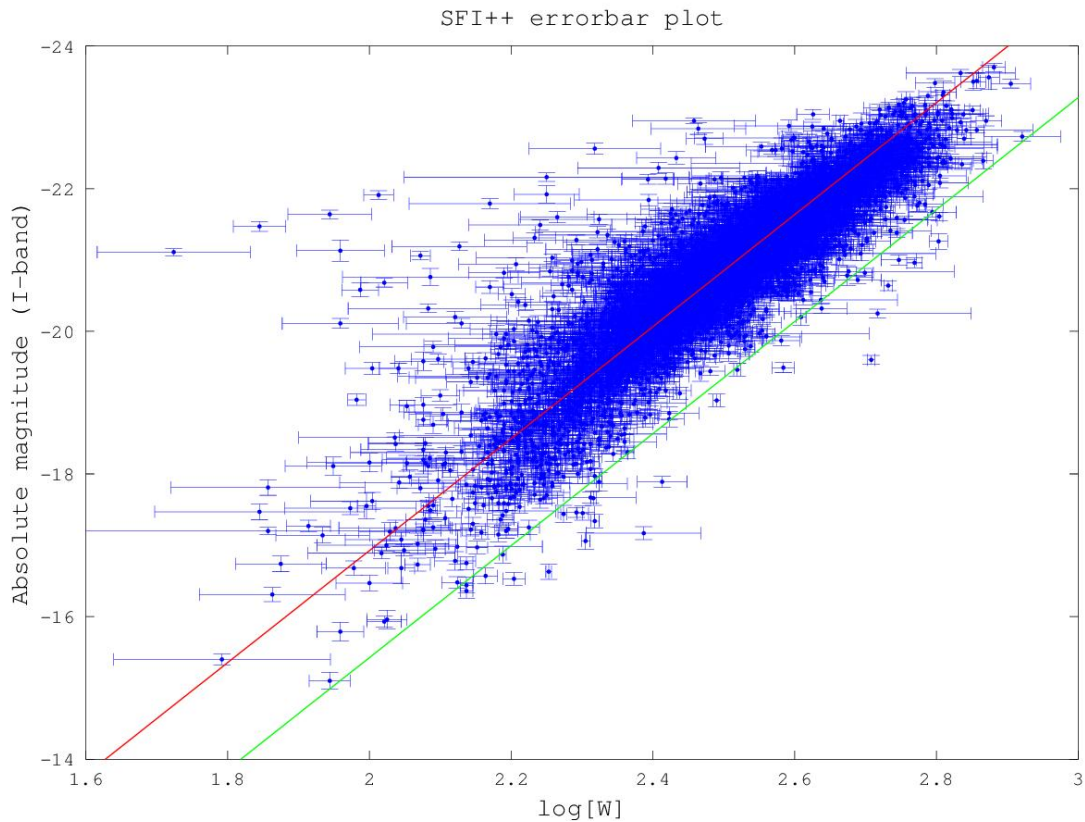


FIGURE 3.3: Plot of the main sample data from the SFI++ catalogue, same as in Fig. 3.2 but with errors in both absolute magnitude and linewidth.

Some extreme outliers were found in Fig. 3.2, both below and above the predicted Tully-Fisher relation. Most of these scattered objects have unusually high uncertainty in line width. This is due to many of them having small inclinations, thus making the corrections to edge-on very large. In their article, Springob et al. (2007) suggests to the readers to make their own cut off in the sample. The advice was kindly taken and all objects with $\log[W] < 2.32$ were removed. The main reason for this rationalizing was because of the huge scattering and downward slope at the lower linewidth, i.e. lower mass. The remaining sample was plotted in Fig. 3.4.

Out of the grand total of 4859 objects, 657 (i.e. 13.5%) objects were removed during the pruning so that 4202 objects remained. 81 of the removed objects were above the fitted TFR red line in Fig. 3.2 whereas 576 were below. Among the remaining sample, 18 (i.e. 0.43%) objects were below the green outlier line in Fig. 3.4 and considered as outliers.

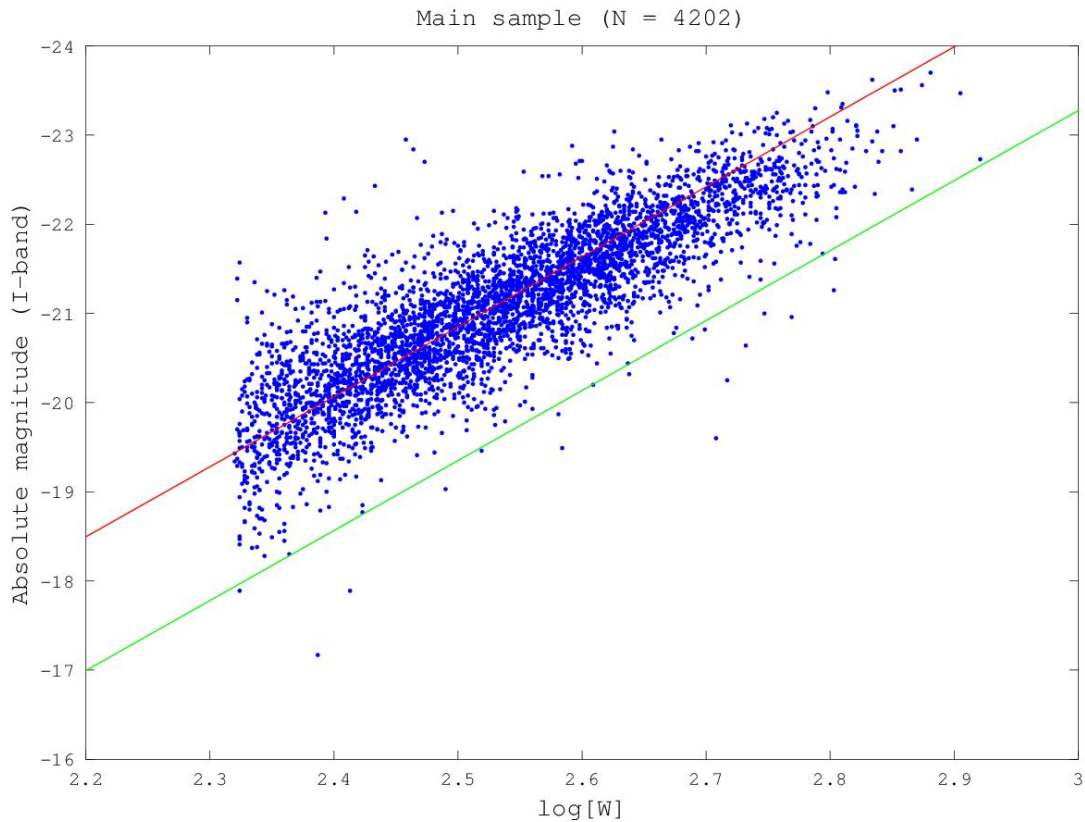


FIGURE 3.4: Plot of the pruned data from the SFI++ catalogue. The Tully-Fisher relation 1.5 is displayed as the red line. The green line 1.5 magnitudes below displays the limit for where outliers are found.

3.3 Intrinsic scatter in the Tully-Fisher relation

As one might note from the various plots so far, the Tully-Fisher relation carries an intrinsic scatter with it. The scatter is somewhat greater at lower linewidth, which can be seen in Fig. 3.2. Masters et al. (2006) used the data from the SFI++ catalogue to fit a width dependent intrinsic scatter to the observed standard deviation from the TFR as

$$\epsilon_{int} = 0.35 - 0.37(\log W - 2.5). \quad (3.1)$$

The scatter is originally assumed to be of Gaussian shape before it is determined. We can use this intrinsic scatter and the observed uncertainties to form a *Monte-Carlo simulation* in order to see how many outliers we expect to get due to random chance.

3.3.1 Monte-Carlo simulation

The simulation was made by randomly distributing 4202 points aligned on the Tully-Fisher relation. The uncertainties from the real data points in the SFI++ catalogue were then altered to a Gaussian distribution and lastly added to the linewidth and the absolute magnitude. The intrinsic scatter from Eq. 3.3 was also added in the same way. The resulting Monte-Carlo simulation is seen in Fig. 3.5 and as a histogram in Fig. 3.6. Repeating the Monte Carlo simulation a number of times yield an average number of 4 outliers.

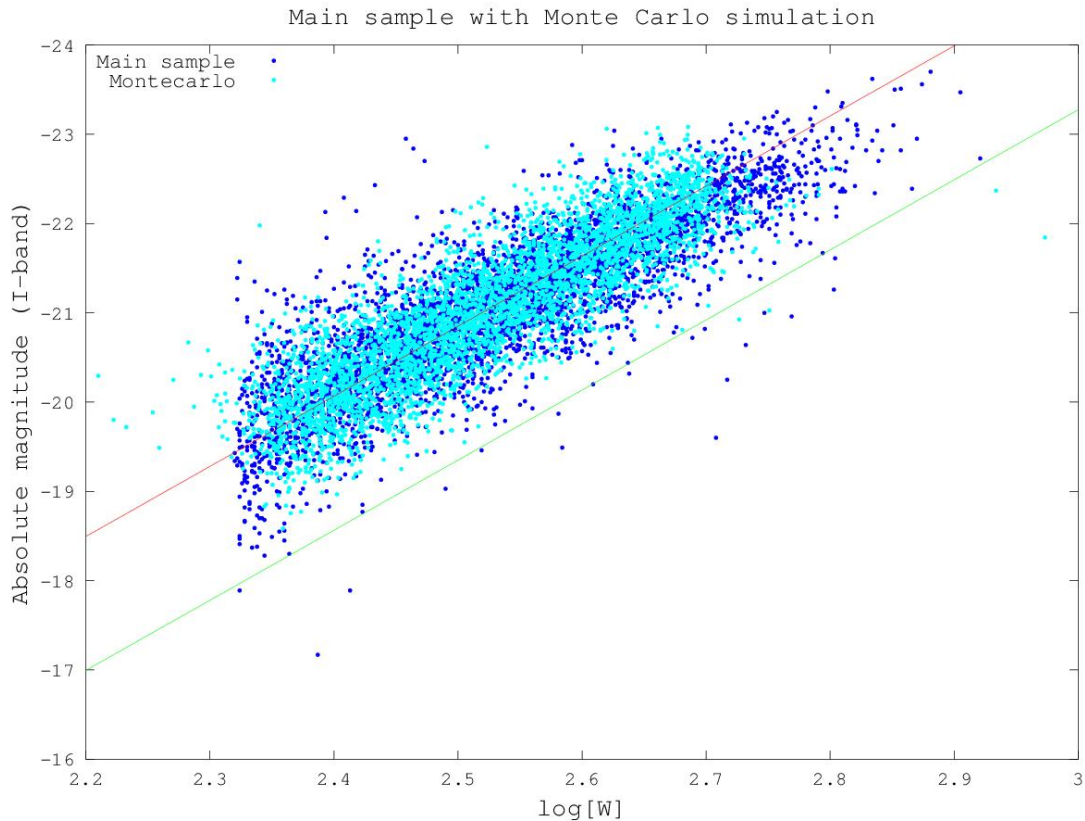


FIGURE 3.5: Monte Carlo simulation of the main sample made by using the intrinsic scatter in the TFR and uncertainties in the observations. Blue dots represent the main sample and cyan dots the simulation. Some points are wandering off to lower linewidth due to their uncertainties.

A *Kolmogorov-Smirnov 2 sample test* was made in order to check whether the two samples could be from the same distribution. In this case, the test showed an average of 1% probability of same distribution and therefore always discarded the null hypothesis that they could be of equal descent. What this indicates is that most of the outliers found are either physical outliers belonging there or due to some catastrophic error estimate (i.e. an error much larger than reflected in the quoted error bars in the original catalogue). The test reveals that the simulation did to reproduce the scatter very well

and the same probability is achieved when we exclude the outliers from the sample and simulation. The test is therefore not sensitive to a few extreme objects, but the outcome is dominated by the shape of the large-scale distribution of the two samples.

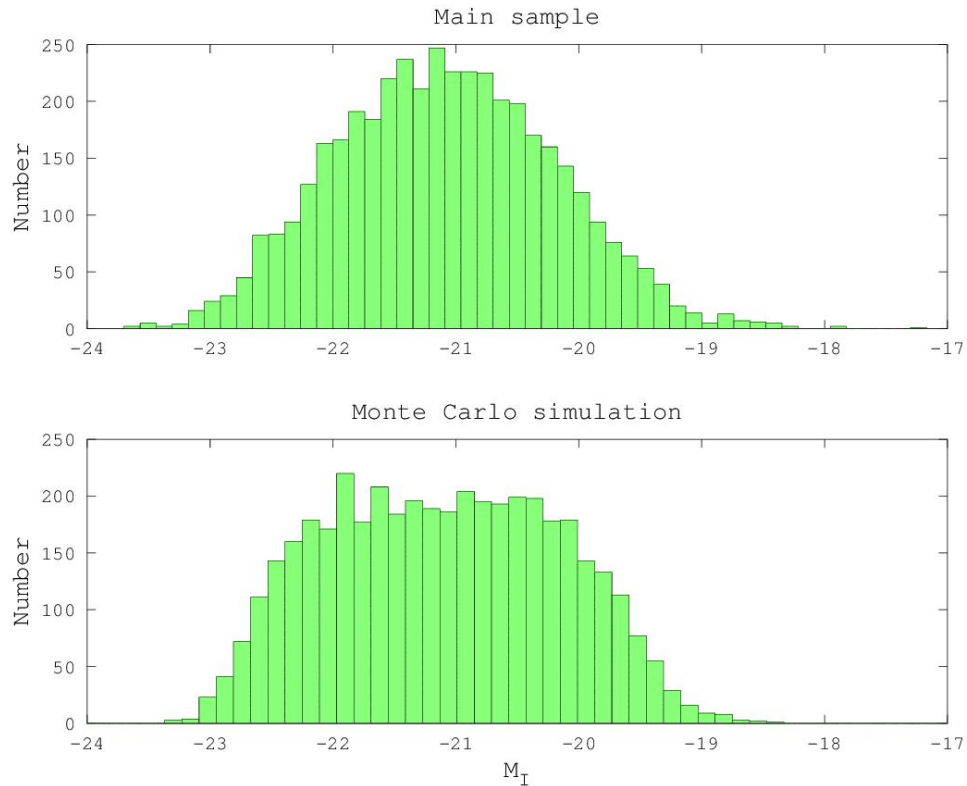


FIGURE 3.6: Upper: Main sample data as a histogram. Lower: Histogram of the the Monte Carlo simulation. M_I is the absolute magnitude in the I-band.

From this we can conclude that a sample of 4202 objects yield an average of 4 outliers (i.e. 0.1%) based on statistical grounds. We can also see from the histogram in Fig. 3.6 that the simulation is much flatter than the real distribution. That is to say, the observed distribution is not well reproduced by intrinsic Gaussian scatter and Gaussian errors.

3.4 Light obstruction

One important factor in determining whether a KIII civilisation would be detectable is the amount of light they let through that we can observe. A limit for outliers is already set at the point where 75% of the light is lost. If only 3/4 of the galaxy is covered by Dyson sphere, it may not necessarily mean the civilisation at hand has achieved full type III status. They would most likely be in a transition state between types II and III. To

gauge this even further, a limit at 90% of the light obscured is set, as well as a limit at 99%. These limits are shown in Fig. 3.7.

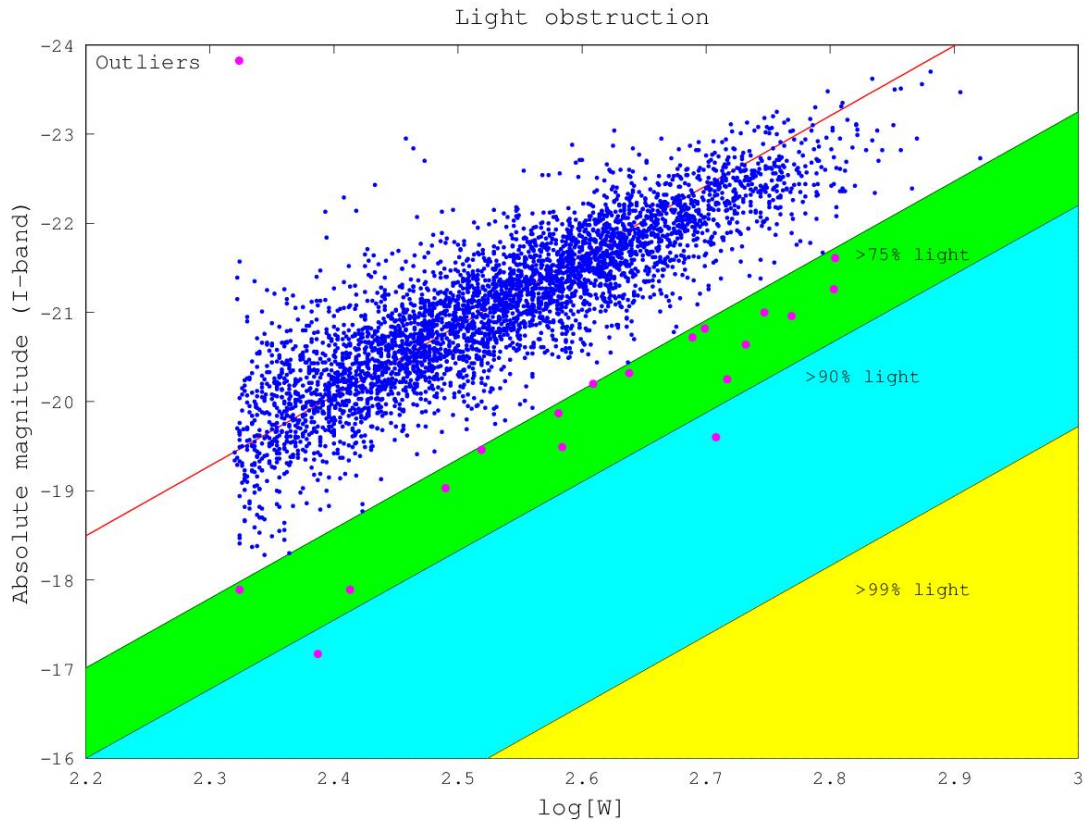


FIGURE 3.7: Limitations for the amount of light obscured is displayed in four layers here. In the green area between 75% and 90% of the light is obscured, in the cyan area between 90% and 99% is obscured and in the yellow area more than 99% of the light is obscured. Magenta coloured dots represents the observed outliers.

Out of our 18 outliers, 2 of them were deemed extreme and found in the zone where more than 90% of the light is obscured. No super-extreme outliers were found in the zone where less than 1% of the light is coming through.

3.4.1 Detection prospects

The restraints of the survey had great impact on where resulting outliers might be found. It was mentioned back in Section 2.2 that the SFI++ catalogue was a compilation of several earlier surveys. One of these surveys had confined objects to be brighter than 14.5 in apparent magnitude. Since there are objects fainter than that in our main sample from the SFI++ catalogue, we have reasons to believe that our results are affected by a selection bias. To correct for this and create a more rigorous search, the apparent magnitude criteria were applied for our entire main sample.

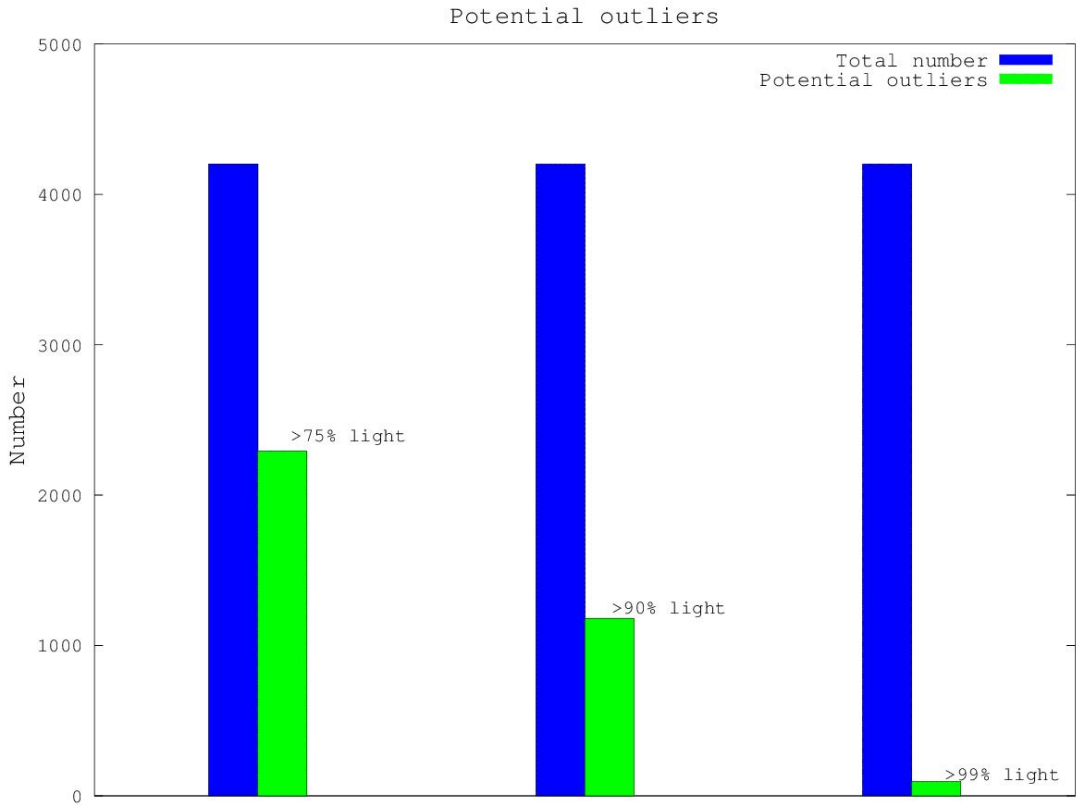


FIGURE 3.8: Bar plot showing the number of potential outlier detections if the limitations are applied to the main sample. Blue bars represents the main sample of 4202 objects and green bars the potential outliers detections at points where more than 75%, 90% and 99% of the light is blocked.

By combining the limitations discussed above and the percentage of light obscured, we could calculate the number of objects that would have been detected had they been actual outliers. This was done by using Eq. 3.4.1 where we define η as the light obscuring coefficient corresponding to 75%, 90% and 99% for the amount of light obscured as 1.5, 2.5 and 5 magnitudes.

$$M_I - (M_{\text{TFR}} + \eta) > m_{\text{app}} - 14.5 \quad (3.2)$$

Here M_I is the absolute magnitude in the I-band, M_{TFR} the absolute magnitude from the TFR, m_{app} the apparent magnitude and 14.5 is the criteria limitation. If the difference on the left side is greater than that of the right hand side, the object would have been detected as an outlier, extreme-outlier or super extreme-outlier. In the main sample, 2411 (i.e 57.4%) could have been detected as outliers with 75% of the light veiled, 1189 (i.e 28.3%) could have been detected with 90% of the light obscured and 95 (i.e 2.3%) could have been detected as super extreme-outliers with > 99% of the light missing. The numbers are compared to the total in a bar plot in Fig. 3.8. This gives us 18 outliers detected out of 2411 possible (i.e 0.66%). Only 2 outliers out of 1189 possible (i.e 0.17%) were detected as extreme outliers when more than 90% of the light

was obscured.

The Monte-Carlo simulation back in Section 3.3.1 showed that approximately 4 outliers out of 4202 objects could be found due to the uncertainties in the observations and the intrinsic scatter in the TFR. When the same simulation is applied for the more rigorous sample of 2411 potential outliers, the average number of outliers is reduced to 2. Better observations with lesser uncertainties should help to bring that number down.

Chapter 4

Results

In this chapter I give more detailed information on the outlying objects deemed as potential Kardashev Type III candidate galaxies and why some were removed from the sample.

4.1 Subsample Outliers

2 outliers were found in the subsample from the Reyes et al. (2011) survey, shown in Table 4.1.

RA	DE	SDSS	M_r	V_{80}	z	In
03 20 19.19	+00 30 05.6	J032019.19+003005.6	81.22	-18.50	0.0234	+
20 35 23.83	-06 14 37.9	J203523.83-061437.9	261.37	-20.53	0.0193	-

TABLE 4.1: Information on the outliers from the subsample. RA and DE are the right ascension and the declination of the galaxies coordinates. M_r is the absolute magnitude in the r-band, V_{80} the rotational velocity at radius 80% from the center and z the redshift. The seventh column "In" displays whether the outlier was kept in the final result by a + sign, or removed, marked with a - sign. All values were corrected in the original compilation as discussed earlier.

4.2 Main Sample Outliers

From the main sample, 2411 objects were used and 18 of them outliers. Outliers with higher quality pictures available are shown in Appendix B. Further information regarding the 18 outliers from the main sample are given in Table 4.2.

RA	DE	Name	$\log[W]$	M_I	cz	Figure	In
00 03 14.8	+16 08 44	N7814	2.708	-19.60	695	B.1	-
00 39 43.1	+09 00 18	409-060	2.717	-20.25	4097	N/A	+
01 43 01.7	+13 38 36	N 660	2.490	-19.03	556	B.2	+
01 50 19.8	+33 09 17	110911	2.747	-21.00	9867	N/A	+
02 08 32.3	+06 19 24	N 825	2.699	-20.82	3130	N/A	+
02 17 53.2	+14 31 16	N 876	2.609	-20.20	3638	N/A	-
02 23 51.9	+25 32 30	483-026	2.689	-20.72	4872	N/A	+
02 39 16.4	+40 52 21	N1003	2.324	-17.89	423	B.3	+
09 19 58.1	+37 11 27	I2461	2.581	-19.87	2495	B.4	-
09 22 02.0	+50 58 39	N2841	2.804	-21.61	803	B.5	+
12 20 38.2	+46 17 30	N4288	2.387	-17.17	5357	B.6	+
12 44 42.6	+40 40 42	I3726	2.769	-20.96	2568	B.7	+
15 15 05.0	+42 12 32	N5900	2.638	-20.32	701	B.8	-
15 33 27.8	+56 33 32	N5963	2.413	-17.89	803	B.9	+
22 00 41.1	+17 44 16	N7177	2.584	-19.49	491	B.10	+
22 37 04.1	+34 24 58	N7331	2.732	-20.64	989	B.11	+
22 37 47.0	+23 47 11	N7339	2.519	-19.46	4687	B.12	+
22 56 50.7	-08 58 03	M-258011	2.803	-21.26	743	B.13	-

TABLE 4.2: Information on the outliers from the main sample. RA and DE are the right ascension and the declination of the galaxies coordinates, M_I the absolute magnitude in the I-band, $\log W$ the base 10 logarithm of the rotational velocity line width and cz the velocity in the Cosmic Microwave Background frame. The eighth column "In" displays whether the outlier was kept in the final result by a + sign, or removed, marked with a - sign. All values were corrected in the original compilation as discussed earlier.

4.3 Final Outliers

Some of the objects found in Tables 4.1 and 4.2 had more conventional explanations for being outliers other than hosting Kardashev type III civilisations.

The second outlier from the sub sample, $J203523.83-061437.9$ in Table 4.1 got discarded due to the object most likely being a falsely made identification by the computerised *SDSS*. In fact, this object is part of another galaxy, *MCG - 01 - 52 - 008*, which is included in the SFI++ catalogue, although not as an outlier. The final number of outliers in the sub sample was then reduced to 1 out of 173 objects (i.e. 0.58%).

From the main sample 5 outliers were removed. Objects N7814, N0876, I2461 and M-258011 were displayed edge-on and got removed due to their inclination most likely

being calculated from the bulge's axis instead of the disk, meaning that the line width was overestimated and the object considered as an outlier. Galaxies viewed edge-on also have the disadvantage that even a small amount of internal absorption can severely affect the deduced structure and parameters because of its long path length throughout the disk. N5900 had a high inclination (almost, if not edge-on) but was also heavily obscured by dust, seen in Fig. B.8. If we take into account the number of outliers in the Monte-Carlo simulation from Section 3.3.1, we can remove an additional 2 outliers based on statistical grounds. This leaves the final number of outliers to 11 out of 2411 observed objects, a portion of 0.46% that meet the criteria for KIII detections discussed in Section 3.4.1.

Some of the outliers found were classified as *lopsided*, meaning they seem to be asymmetric in shape. For a lopsided galaxy, one side of the disk is more massive or more extended than the other side. Although usually a trait for low luminous and late type spiral galaxies as explained by Zaritsky et al. (2013), it is also an attribute one might expect from a galaxy hosting a civilisation that is making Dyson spheres in larger parts of the galaxy. For example, if colonization is starting on one side of the disk making it appear darker, an observer would think the nucleus is shifted towards that side of the disk. A galaxy where half of the disk is unseen would indeed create the visual illusion of being lopsided.

Chapter 5

Conclusions

Here I present my resulting findings and discuss them. I also calculate the maximum rate of star-fed type III civilisations observed and discuss error sources. Only the main sample's results are used in the calculations as the smaller r-band sample from Reyes et al. (2011) is not large enough to provide competitive constraints. With its more stringent selection criteria, it does however, serve as a consistency check.

5.1 The rate of star-fed type III civilisations

A lower limit to the time scale for a galaxy to become part of a star-fed Kardashev type III civilisation was determined by Annis (1999). The same procedure is mimicked here but with the data from our main sample instead. Out of 31 spiral galaxies Annis (1999) found no potential KIII candidates, whereas here 11 are found out of a sample of 2411 galaxies. This translates into 3.23% and 0.46% for the upper limit of the observed spiral disk galaxies to host a star fed KIII civilisation.

Assuming that a KIII civilisation may rise at any given time in history *i.e.*, a random process characterised by a constant probability of occurrence per unit time. Then a Poissonian probability p for zero occurrences in time T is

$$p = \exp^{-rT} \tag{5.1}$$

where r is the rate of rise of KIII civilisations. Using the Milky Way as a baseline and integrating over 10 billion years no type III civilisations were found. Had there been any in the galaxy, we would most likely have known about it. Annis (1999) argues that giving this zero-occurrence happening by random a 1% probability, the rate of rise of

KIII civilisations is $r < 4.6 \times 10^{-10}/\text{yr}$. At the 99% confidence level the lower limit to characteristic time-scale for the rise of KIII civilisations is $r^{-1} \leq 2$ billion years.

For this zero-occurrence to fail to happen for the probability gained here, $p = (1-0.0046)$, the rate of rise would be $r < 4.6 \times 10^{-13}$. This translates into a characteristic time-scale for the rise of KIII civilisations to $r^{-1} \geq 2.2 \times 10^{12}$ years, far above the age of the Universe of 13.80 Gyr. (Planck Collaboration, Ade et al. 2013).

5.2 Uncertainties

The final number of outliers and potential type III Kardashev civilisations gained here may be 11, but this figure is clouded with uncertainty. As explained in Section 3.4.1 and the criteria of certain surveys, many potential outliers goes unspotted. The Reyes (2011) survey absolute magnitude criteria exclude any low luminous fainter than -18 absolute magnitude. Even the Sérsic index criteria may boot out objects of interest if a potential KIII civilisation engulfs a number of stars in Dyson spheres and thus changing the Sérsic index. In similar ways, if a type III civilisation darken a great part of the major axis of a galaxy, the corrected linewidth may be overestimated. The same argument goes for underestimating the linewidth if the minor axis is altered and a type III civilisation shows up within the limit not to be considered as an outlier. Errors in the inclination of the surveys work in two ways; if the axis ratio (minor- over major axis, b/a) of the observed galaxy is larger than the real value, the inclination correction is overestimated and the uncertainty in linewidth increases. On the other hand, if the axis ratio is calculated to be too low, then the correction to extinction when calculating the absolute magnitude is underestimated.

Another source of uncertainty is the possibility of an outlier being a luminous infrared galaxy. Such a galaxy emits a large majority of its bolometric luminosity in the far infrared while otherwise obscured. LIRGs are generally found in merger or interacting systems where lots of dust and gas gather towards the nucleus (Lahuis et al. 2007). They may also contain a stronger star formation rate than most galaxies, making them *starburst galaxies*. The forming of massive young stars contribute to strong luminosity in the ultraviolet but because of the dusty environment it may not always be seen. The dust in that case absorbs the UV radiation and re-radiates it at longer wavelengths (Howell et al. 2010). A galaxy hosting a KIII civilisation that has most of the stars enclosed in Dyson spheres would also show up as a luminous object in the far infrared as discussed in Section 1.3. This makes LIRGs quite alluring objects when searching for Kardashev type III civilisations, due to possessing the same properties that is being sought. Out of the outliers found, only 1 was classified as a LIRG and is seen in Fig. B.2.

Setting up a Dyson sphere around a star is not the only usage of a Dysonian construction to extract an immense amount of energy. The possibility of constructing a Dyson sphere or setting up several power plants around a *super-massive black hole* has been discussed by Inoue & Yokoo (2011). Taking advantage of the SMBH accretion disk would be more difficult than the stellar Dyson sphere model, but the reward greater as well. Doing so would not necessarily affect the luminosity of the galaxy either, so they would not be detected as an outlier in a search such as this one. Nevertheless, a civilisation or galactic club capable of constructing a Dyson sphere around their galaxy's SMBH would probably have tested out the fundamentals on a star or two first, not inevitably many.

5.3 Discussion

It is quite hard to argue for how many Kardashev type III civilisations there are in the entire Universe. Sure, we found here from our sample of 4202 spiral galaxies that roughly 1 in 250 break the natural scaling laws for mass and luminosity, but also that some of the galaxies that do so are simply because of errors in the observations. An outlier does not necessarily mean that the galaxy in question is hosting a KIII civilisation, merely that it *is* an interesting object that *may* be explained by such.

In Section 3.4.1 we included a criteria for our sample that all objects had to be detectable as outliers in order to stay in the sample. Almost half the sample was lost in favour of a more strict sample than before, where we knew exactly how many objects could have been detected as outliers had they been dimmed out. Had we not done so and kept the larger sample of 4202 objects, the uncertainty in the the number of outliers would have risen. We would then not have known how many outliers went undetected due to being too faint.

Given the data at hand and using the technique provided by Annis (1999), we expect the upper limit of KIII candidates to be $\approx 1/220$. The number of outliers can easily go up or down depending on where one sets the limit for determining an outlier. If we set the detection limit at 90% of the light obscured, only 1 outlier is found out of 1180 detectable objects. If we instead set the detection limit at 99% of the light obscured, no outlier is found and the sample is reduced to 95 objects detectable as such. Also considering the downward slope and the intrinsic scatter in the TFR, which according to Masters et al. (2006) is larger for low-mass spiral galaxies, makes the technique vulnerable to where one places the detection limit. Too close to the TFR and the number of outliers gets overestimated, too far away and not enough objects are detectable to give conclusive results. The technique is thus more suitable for spiral disk galaxies with moderate or

high mass. Here, the issue was resolved by removing all objects below a certain rotational velocity line width until the downward slope and scatter diminished.

The fraction of outliers from consistency check subsample of the Reyes (2011) data agreed rather well with the main sample. The subsample yielded a fraction of 1/173 as compared to the main sample's 1/220. Had the differences been too large, one could have suspected the criteria and size of the samples as the reason. By applying the same criteria of absolute magnitude being between -18 and -22.5 for our main sample, we actually get 1/246 objects to be Kardashev type III civilisation candidates. Nevertheless, we are in fact looking for objects fainter than the suggested standard, thus making surveys with such absolute magnitude criteria undesirable. The size of the sample presented here is 14 times larger than the subsample and almost 80 times larger than the one Annis (1999) used, implying a greater statistical power.

Our sample of data was confined to quite small distances and low redshift, which is more optimal when searching for extraterrestrial intelligence. With greater distance on cosmic scales comes greater redshift, meaning a greater look-back time. In other words, a galaxy *far far away* would also imply a time *long long ago*. This should not affect our search very much, as the redshift is restricted to $z < 0.1$ where the effect is very small. Although the rise from a type 0 to a type III civilisation should require some time, a Kardashev type III civilisation should not be able to rise before the hosting galaxy formed planets. So by looking at a galaxy when it was much younger, its population may not have developed into what it is today and therefore we expect more KIII civilisations to be detected at low redshift. This also coincides with our results where the outliers have a mean redshift of $\bar{z} \approx 0.009$ whereas the full sample has $\bar{z} \approx 0.017$. However, this difference in redshift corresponds to roughly 100 million years with current Cosmology ($H_0 = 67.8$, $\Omega_M = 0.32$, $\Omega_\Lambda = 0.68$). A time span which is hardly enough to colonize an entire galaxy unless they can capture stars with near relativistic speeds. In other words, we do not expect there to be any significant difference in number of outliers at this low redshift, and the discrepancy in redshift here is negligible.

Although we only have ourselves and our ancestors as a comparison, our modern civilisation has only been around for a brief moment whereas a civilisation that has achieved type III status may persevere for a much longer time as no natural disasters can threaten them. That is to say, once a civilisation has ascended up the Kardashev scale, they will continue colonising the galaxy, completely encasing all the stars and remain hidden from outsiders for a very long time.

For future works I recommend looking further into the outliers found here, conceivably testing ones fortune with *Lucky Imaging*. By taking many consequently pictures fast enough to freeze the motion of turbulence in the atmosphere, some of them may be

sufficiently sharp for usage. Applying different photometric filters and comparing them could be used to see if there are any suspicious differences. For instance, a black fissure or void could point to a type II civilisation on the rise assembling Dyson spheres. When analysing the total spectrum of a galaxy a spectral synthesis model can be used to make certain assumptions about the stellar initial mass function. A galaxy filled with Dyson spheres may break from the estimated model, resulting in an oddly shaped total spectrum which does not necessarily mimic that of something with a large dust content. A targeted search in the deep infrared may perhaps put some better perspective on the outliers' dim nature. I also propose resorting to a larger sample than the one exhibited here, with better limitations on the observations e.g. being able to see fainter objects.

5.4 Summary

We started with a sample of 4859 spiral disk galaxies from the SFI++ catalogue which were plotted in Tully-Fisher diagrams in order to search for galaxies that broke the natural scaling laws between luminosity and mass. Due to the scatter in the TFR being higher at the low mass end, a criteria of $\log[W] > 2.32$ was applied so that 4202 objects remained. Using the technique innovated by Annis (1999), a limit 1.5 magnitudes below the Tully-Fisher relation was applied where objects were considered as outliers and potential Kardashev type III candidates. In this case 18 outliers were found.

Limitations and criteria from the original literature caused a bias of including many objects that would not have been detected had their luminosities been dimmed out. To correct for this an additional criteria was established as Equation 3.4.1 and the number of detectable objects as potential outliers was calculated in Section 3.4.1. The remaining sample of 2411 objects were all capable of being detected had their luminosities been darkened by 75%. The procedure was repeated for higher fractions of light obstruction at 90% and 99%, corresponding to 2.5 and 5 magnitudes below the TFR. Only 2 outliers were found more than 2.5 magnitudes below the TFR where 1189 objects were detectable. 95 objects were detectable 5 magnitudes below the TFR but no such super-extreme outlier was found.

The 18 outliers were investigated more closely until 5 of them could be explained by more orderly means, mostly due to being viewed edge-on but miscalculated for such in the original literature. A Monte-Carlo simulation was made as well in order to see how many outliers were due to statistical errors and intrinsic scatter in the TFR. The Monte-Carlo simulation reproduced on average 0.01% of the simulated data as outliers.

We also laid down some limitations to the technique selected for the search. Primarily, one has to assume that highly advanced and intelligent Kardashev type III civilisations are utilizing Dyson spheres around stars to support their energy consumption. Another issue that occurs is the 1.5 magnitude limit may overestimate the number of outliers due to the intrinsic scatter and downward trend in the low rotational velocity (i.e. mass) end of the TFR. It can be solved by inserting minimum rotational velocity criteria, but that reduces the amount of objects all in all. Making a limit that is dependent of the scatter may adjust the limitations of this technique. It should be added that the technique may be used more efficiently with the baryonic TFR, where the intrinsic scatter is somewhat smaller (McGaugh 2000). One great advantage of the technique in question is that it does not require any new observations to utilize. Compiling data from literature is a viable method as shown here.

The main goal of this search was to produce a better upper limit for the amount of Kardashev type III civilisation we can observe than that advertised by Annis (1999). After applying the corrections for a more rigorous search, removing the 5 outliers that had conventional explanations and an additional 2 outliers due to statistical grounds, only 11 outliers out of 2411 objects remained (i.e. 0.46%). Comparing this to the old upper limit set by Annis (1999) of 3.2%, the goal was achieved and the upper limit reduced by nearly a full order of magnitude!

Appendix A

Final sample

Histograms of the data used in the full and final main sample are shown in Fig. A.2. Rotational velocity line widths along with apparent and absolute magnitudes were obtained directly from the literature. Distances were calculated using the distance modulus

$$M_{abs} = m_{app} - 5 \cdot \log\left(\frac{d}{10\text{pc}}\right) + 5 \quad (\text{A.1})$$

where d is the distance in Mpc, which with some algebra can be assessed as

$$d = 10^{\frac{m_{app} - M_{abs}}{5} + 1}.$$

The final sample of objects is plotted in a Tully-Fisher diagram in Fig. A.1.

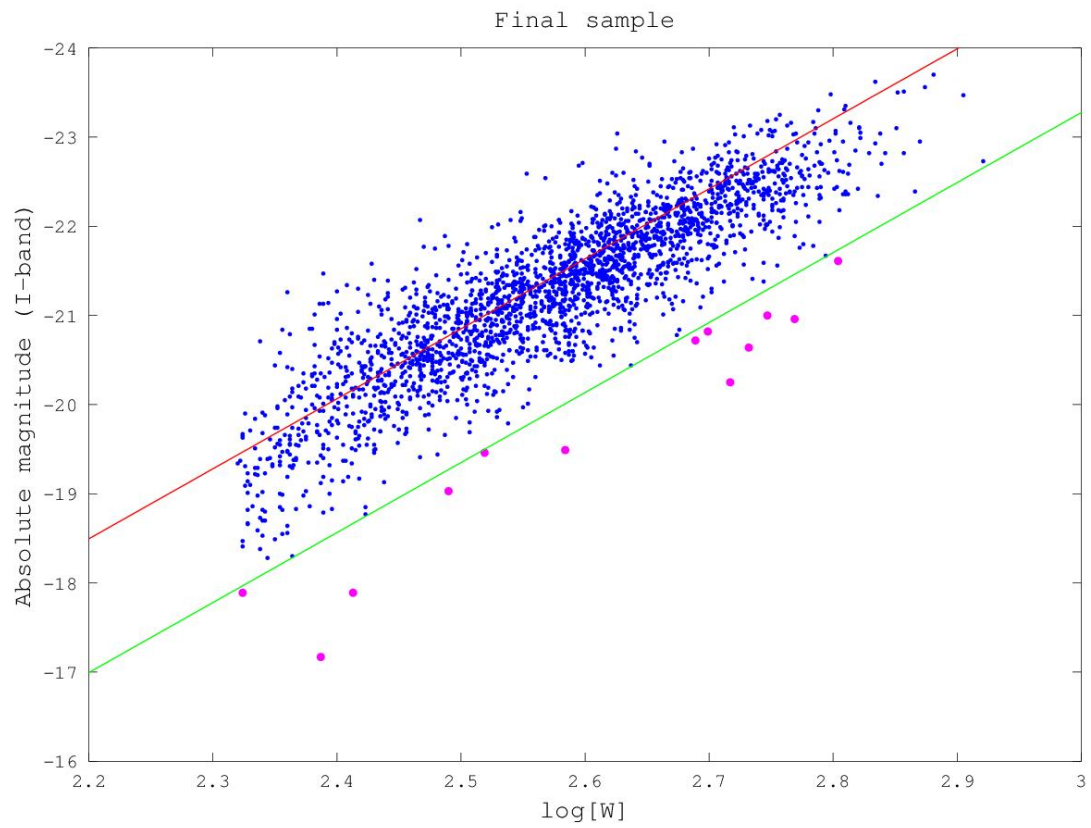


FIGURE A.1: Tully-Fisher diagram of the final sample. Outliers removed from the final results were also withdrawn from the plot.

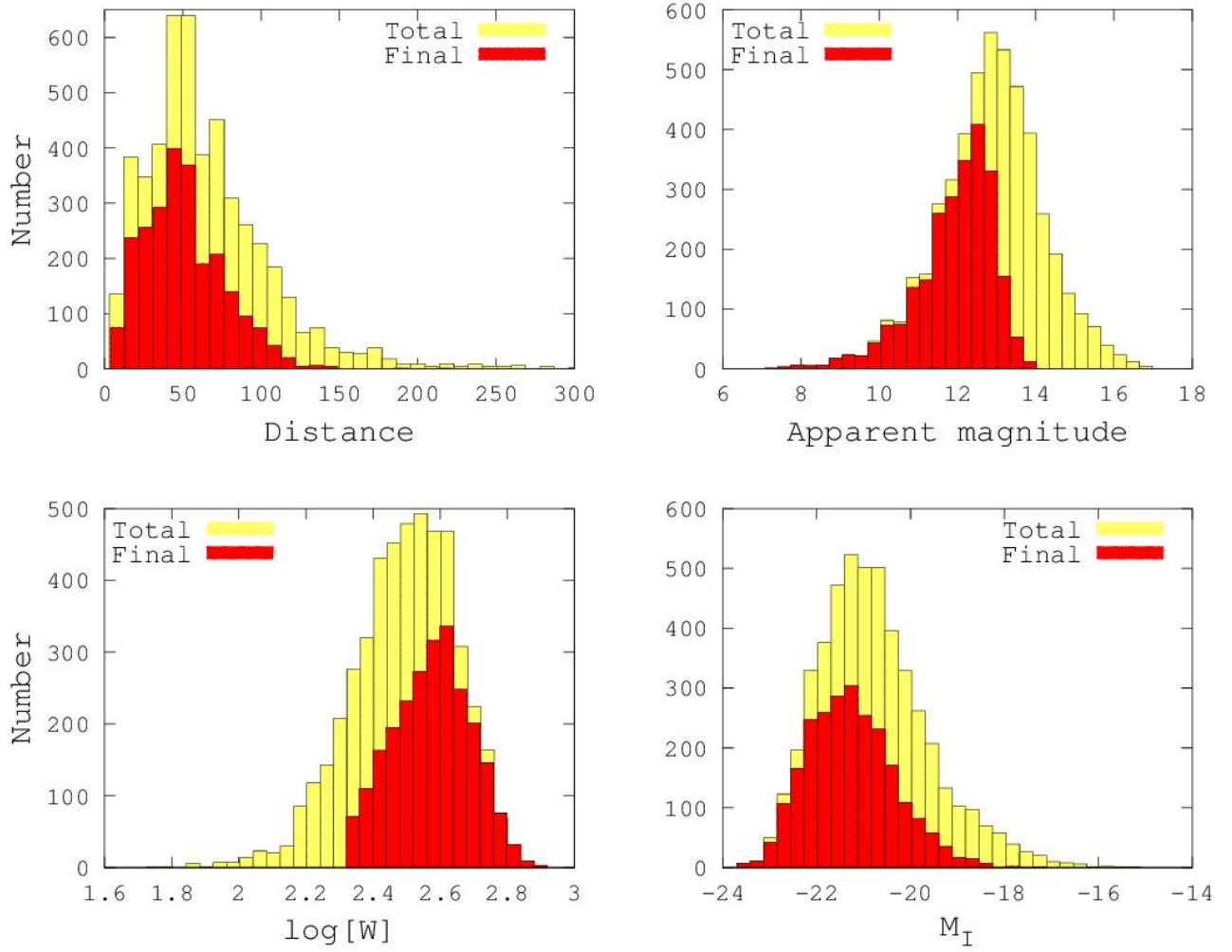


FIGURE A.2: Histograms of distances in Mpc, apparent magnitudes, rotational velocity line widths $\log[W]$ and absolute magnitudes M_I from the main sample. Yellow bars show the full original sample and red bars the final sample.

Appendix B

Galaxies

Images and small descriptions of some of the outliers from Tables. 4.1 & 4.2 are displayed in this appendix.

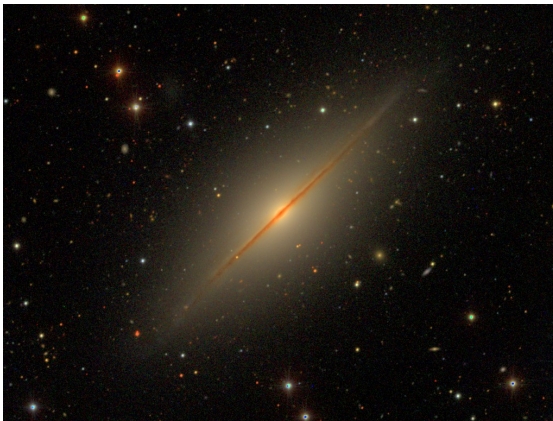


FIGURE B.1: NGC 7814. Size 10.9 x 10.9 arcmin. Photometry gri. A galaxy from the outlier group discarded from the final sample, displayed edge-on.



FIGURE B.2: NGC 0660. Size 16.6 x 16.6 arcmin. Photometry gri. A galaxy from the outlier group kept in the final sample, deemed as a LIRG and starburst galaxy.



FIGURE B.3: NGC 1003. A galaxy from the outlier group kept in the final sample. Considered as lopsided.

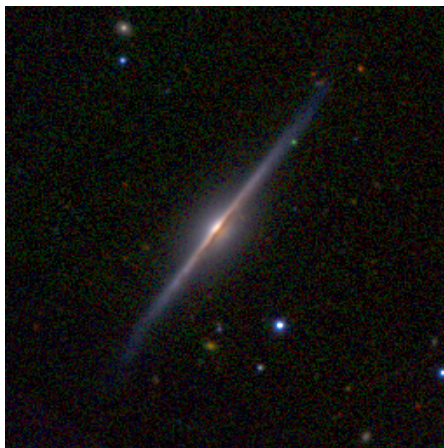


FIGURE B.4: IC 2461. Size 4.7 x 4.7 arcmin. Photometry gri. A galaxy from the outlier group discarded from the sample, displayed edge-on.

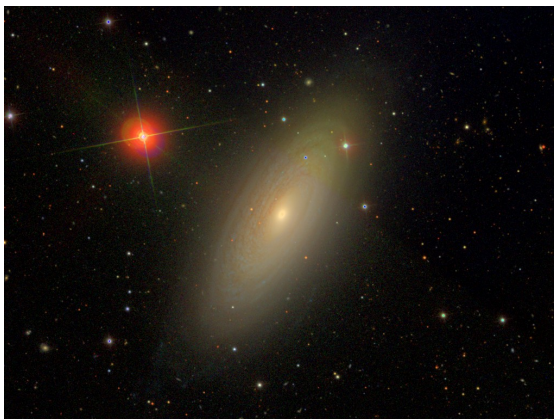


FIGURE B.5: NGC 2841. Size 10.4 x 10.4 arcmin. Photometry gri. A galaxy from the outlier group kept in the final sample.

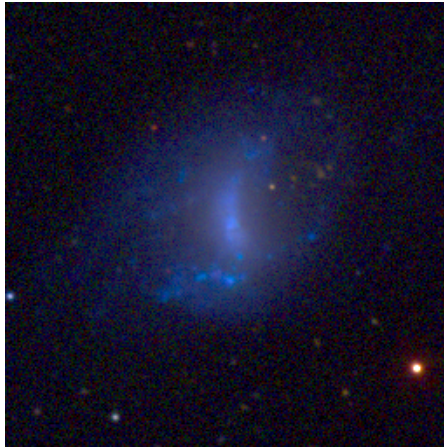


FIGURE B.6: NGC 4288. Size 4.3 x 4.3 arcmin. Photometry gri. One of the extreme outlier galaxies kept in the final sample.

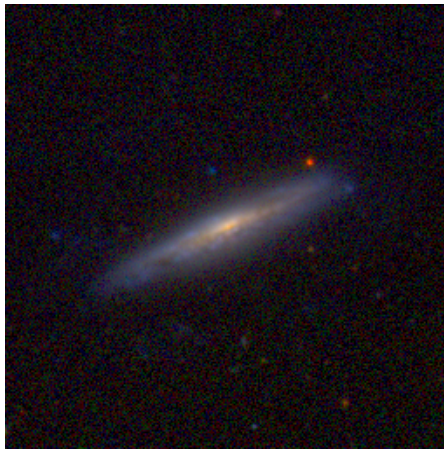


FIGURE B.7: IC 3726. Size 2.9 x 2.9 arcmin. Photometry gri. One of the outlier galaxies kept in the final sample.

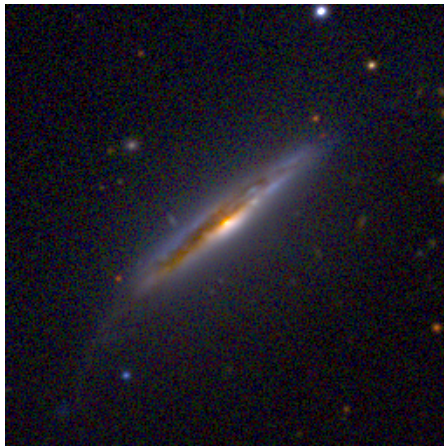


FIGURE B.8: NGC 5900. Size 3.3 x 3.3 arcmin. Photometry gri. A galaxy from the outlier group displayed edge-on, discarded from the final batch.



FIGURE B.9: NGC 5963. Photometry gri. One of the outlier galaxies kept in the final sample.



FIGURE B.10: NGC 7177. Photometry B,V and R filters. One of the outlier galaxies kept in the final sample.



FIGURE B.11: NGC 7331. Size 0.23 arcsec per pixel. Photometry LRGB. A galaxy from the outlier group kept in the final sample. Considered as a liner and lopsided.

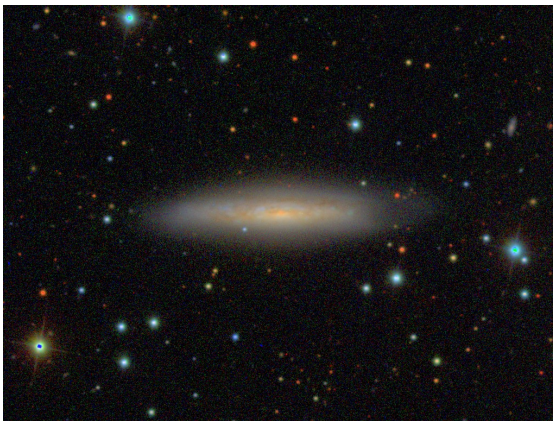


FIGURE B.12: NGC 7339. Photometry gri. One of the outlier galaxies kept in the final sample.

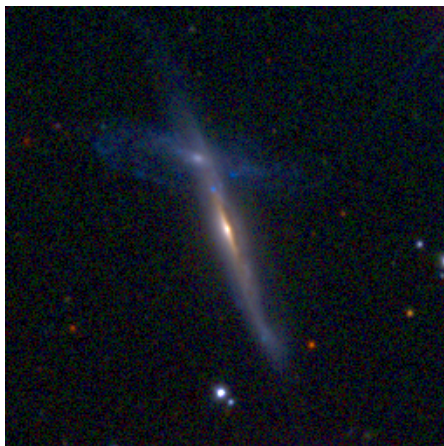


FIGURE B.13: M-258011. Size 4.0 x 4.0 arcmin. Photometry gri. One of the outlier objects discarded from the final sample. Most likely two galaxies interacting, M-258011 and M-258012.

Bibliography

- Annis, J. (1999). Placing a limit on star-fed Kardashev type III civilisations. *Journal of the British Interplanetary Society*, 52:33–36.
- Backus, P. R. and Project Phoenix Team (2004). Project Phoenix: A Summary of SETI Observations and Results, 1995 - 2004. In *American Astronomical Society Meeting Abstracts #204*, volume 36 of *Bulletin of the American Astronomical Society*, page 805.
- Bowyer, S. (2011). *SERENDIP: The Berkeley SETI Program*, page 99.
- Bowyer, S., Werthimer, D., Donnelly, C., Lampton, M., Herrick, W., Soller, J., Ng, D., and Hiatt, T. (1993). The SERENDIP SETI Project. In Shostak, G. S., editor, *Third Decennial US-USSR Conference on SETI*, volume 47 of *Astronomical Society of the Pacific Conference Series*, page 269.
- Burstein, D., Haynes, M. P., and Faber, M. (1991). Dependence of galaxy properties on viewing angle. *Nature*, 353:515–521.
- Carrigan, Jr., R. A. (2009). IRAS-Based Whole-Sky Upper Limit on Dyson Spheres. *The Astrophysical Journal*, 698:2075–2086.
- Cocconi, G. and Morrison, P. (1959). Searching for Interstellar Communications. *Nature*, 184:844–846.
- Courteau, S. (1997). Optical Rotation Curves and Linewidths for Tully-Fisher Applications. *The Astrophysical Journal*, 114:2402.
- Drake, F. D. (1961). Project Ozma. *Physics Today*, 14:40–46.
- Dyson, F. J. (1960). Search for Artificial Stellar Sources of Infrared Radiation. *Science*, 131:1667–1668.
- Freitas, Jr., R. A. (1980). A self-reproducing interstellar probe. *Journal of the British Interplanetary Society*, 33:251–264.

- Giovanelli, R., Haynes, M. P., Salzer, J. J., Wegner, G., da Costa, L. N., and Freudling, W. (1994). Extinction in SC galaxies. *The Astrophysical Journal*, 107:2036–2054.
- Guth, A. (1997). Cooking up a cosmos. *Astronomy*, 25:54–57.
- Howell, J. H., Armus, L., Mazzarella, J. M., Evans, A. S., Surace, J. A., Sanders, D. B., Petric, A., Appleton, P., Bothun, G., Bridge, C., Chan, B. H. P., Charmandaris, V., Frayer, D. T., Haan, S., Inami, H., Kim, D.-C., Lord, S., Madore, B. F., Melbourne, J., Schulz, B., U, V., Vavilkin, T., Veilleux, S., and Xu, K. (2010). The Great Observatories All-sky LIRG Survey: Comparison of Ultraviolet and Far-infrared Properties. *The Astrophysical Journal*, 715:572–588.
- Inoue, M. and Yokoo, H. (2011). Type III Dyson Sphere of Highly Advanced Civilisations around a Super Massive Black Hole. *Journal of the British Interplanetary Society*, 64:59–62.
- Kardashev, N. S. (1964). Transmission of Information by Extraterrestrial Civilizations. *Sovjet Astronomy*, 8:217.
- Lahuis, F., Spoon, H. W. W., Tielens, A. G. G. M., Doty, S. D., Armus, L., Charmandaris, V., Houck, J. R., Stäuber, P., and van Dishoeck, E. F. (2007). Infrared Molecular Starburst Fingerprints in Deeply Obscured (Ultra)Luminous Infrared Galaxy Nuclei. *The Astrophysical Journal*, 659:296–304.
- Masters, K. L., Springob, C. M., Haynes, M. P., and Giovanelli, R. (2006). SFI++ I: A New I-Band Tully-Fisher Template, the Cluster Peculiar Velocity Dispersion, and H_0 . *The Astrophysical Journal*, 653:861–880.
- Masters, K. L., Springob, C. M., and Huchra, J. P. (2008). 2MTF. I. The Tully-Fisher Relation in the Two Micron all Sky Survey J, H, and K Bands. *The Astronomical Journal*, 135:1738–1748.
- McGaugh, S. S., Schombert, J. M., Bothun, G. D., and de Blok, W. J. G. (2000). The Baryonic Tully-Fisher Relation. *The Astrophysical Journal*, 533:L99–L102.
- Pizagno, J., Prada, F., Weinberg, D. H., Rix, H.-W., Pogge, R. W., Grebel, E. K., Harbeck, D., Blanton, M., Brinkmann, J., and Gunn, J. E. (2007). The Tully-Fisher Relation and its Residuals for a Broadly Selected Sample of Galaxies. *The Astronomical Journal*, 134:945–972.
- Planck Collaboration, Ade, P. A. R., Aghanim, N., Armitage-Caplan, C., Arnaud, M., Ashdown, M., Atrio-Barandela, F., Aumont, J., Baccigalupi, C., Banday, A. J., and et al. (2013). Planck 2013 results. XVI. Cosmological parameters. *ArXiv e-prints*.

- Reyes, R., Mandelbaum, R., Gunn, J. E., Pizagno, J., and Lackner, C. N. (2011). Calibrated Tully-Fisher relations for improved estimates of disc rotation velocities. *Monthly Notices of the Royal Astronomical Society*, 417:2347–2386.
- Riess, A. G., Filippenko, A. V., Challis, P., Clocchiatti, A., Diercks, A., Garnavich, P. M., Gilliland, R. L., Hogan, C. J., Jha, S., Kirshner, R. P., Leibundgut, B., Phillips, M. M., Reiss, D., Schmidt, B. P., Schommer, R. A., Smith, R. C., Spyromilio, J., Stubbs, C., Suntzeff, N. B., and Tonry, J. (1998). Observational Evidence from Supernovae for an Accelerating Universe and a Cosmological Constant. *The Astronomical Journal*, 116:1009–1038.
- Rubin, V. C., Burstein, D., Ford, Jr., W. K., and Thonnard, N. (1985). Rotation velocities of 16 SA galaxies and a comparison of Sa, Sb, and SC rotation properties. *The Astrophysical Journal*, 289:81–98.
- Schlegel, D. J., Finkbeiner, D. P., and Davis, M. (1998). Maps of Dust Infrared Emission for Use in Estimation of Reddening and Cosmic Microwave Background Radiation Foregrounds. *The Astrophysical Journal*, 500:525.
- Shuch, H. P. (2011). *Project Argus: Pursuing Amateur All-Sky SETI*, page 201.
- Springob, C. M., Haynes, M. P., Giovanelli, R., and Kent, B. R. (2005). A Digital Archive of H I 21 Centimeter Line Spectra of Optically Targeted Galaxies. *The Astrophysical Journal Supplement Series*, 160:149–162.
- Springob, C. M., Masters, K. L., Haynes, M. P., Giovanelli, R., and Marinoni, C. (2007). SFI++. II. A New I-Band Tully-Fisher Catalog, Derivation of Peculiar Velocities, and Data Set Properties. *The Astrophysical Journal Supplement Series*, 172:599–614.
- Strauss, M. A. and Willick, J. A. (1995). The density and peculiar velocity fields of nearby galaxies. *Physics Reports*, 261:271–431.
- Tarter, J. (2001). The Search for Extraterrestrial Intelligence (SETI). *Annual Review of Astronomy and Astrophysics*, 39:511–548.
- Tully, R. B. and Fisher, J. R. (1977). A new method of determining distances to galaxies. *Astronomy and Astrophysics*, 54:661–673.
- Tully, R. B., Pierce, M. J., Huang, J.-S., Saunders, W., Verheijen, M. A. W., and Witchalls, P. L. (1998). Global Extinction in Spiral Galaxies. *The Astronomical Journal*, 115:2264–2272.
- Zaritsky, D., Salo, H., Laurikainen, E., Elmegreen, D., Athanassoula, E., Bosma, A., Comerón, S., Erroz-Ferrer, S., Elmegreen, B., Gadotti, D. A., Gil de Paz, A., Hinz,

J. L., Ho, L. C., Holwerda, B. W., Kim, T., Knapen, J. H., Laine, J., Laine, S., Madore, B. F., Meidt, S., Menendez-Delmestre, K., Mizusawa, T., Muñoz-Mateos, J. C., Regan, M. W., Seibert, M., and Sheth, K. (2013). On the Origin of Lopsidedness in Galaxies as Determined from the Spitzer Survey of Stellar Structure in Galaxies (S4G). *ArXiv e-prints*.